Structure of Symmetric and Asymmetric "Ripple" Phases in Lipid Bilayers

Olaf Lenz and Friederike Schmid
Fakultät für Physik, Universität Bielefeld, D-33615 Bielefeld, Germany
(Received 3 August 2006; published 30 January 2007)

We reproduce the symmetric and asymmetric "rippled" $P_{\beta'}$ states of lipid membranes by Monte Carlo simulations of a coarse-grained molecular model for lipid-solvent mixtures. The structure and properties compare favorably with experiments. The asymmetric ripple state is characterized by a periodic array of fully interdigitated "defect" lines. The symmetric ripple state maintains a bilayer structure, but is otherwise structurally similar. The main force driving the formation of both ripple states is the propensity of lipid molecules with large head groups to exhibit splay.

DOI: 10.1103/PhysRevLett.98.058104 PACS numbers: 87.16.Dg, 82.70.Uv, 87.14.Cc, 87.16.Ac

Membranes are ubiquitous in all living organisms [1]. Their central structural element is a lipid bilayer, which is stabilized by the amphiphilic character of lipid molecules: they self-assemble such that their hydrophilic head groups shield the hydrophobic tails from the surrounding water. Pure lipid bilayers have been studied for a long time as model systems that can provide insight into the structural properties of biomembranes. Already these seemingly simple systems exhibit a rich spectrum of structures and phase transitions [2–5]. The most common state in nature is the so-called "fluid" state (L_α), which is characterized by a large number of chain defects and high lipid mobility. If one decreases the temperature, one encounters a phase transition (the "main" transition) to a "gel" state where the lipid molecules are more ordered and less mobile. The structure of this low temperature phase depends on the interactions between the lipid head groups. Loosely speaking, lipids with small head groups such as phosphatidylethanolamines [4] assume a state where the long axes of the chains remain perpendicular to the bilayer normal (L_β phase). Lipids with large head groups and relatively strong head-head attraction such as phosphatidylcholines [5] exhibit tilt ($L_{\beta'}$ phase). Finally, lipids with large head groups and weak head-head attraction such as ether linked phosphatidylcholines [5,6] form a phase L_β^{int} where both opposing lipid layers are fully interdigitated [4,5].

The main transition has attracted considerable interest, since it occurs at temperatures that are typical on Earth (between -20 and 60 °C). The mechanism that governs the transition $L_\alpha \leftrightarrow L_\beta$ to the untilted gel is comparatively straightforward. The transition is driven by the competition of the entropy of chain disorder and the free energy of chain alignment [7,8] (i.e., chain packing) and is thus in some sense related to the isotropic-nematic transition of liquid crystals. At the transition $L_\alpha \leftrightarrow L_{\beta'}$ to the tilted gel, the situation is much more complicated. Here, the main transition is preempted by a "pretransition," and one observes an intermediate state with a periodic, wavelike surface structure: The "ripple" phase $P_{\beta'}$, first reported by Tardieu *et al.* [9]. The microscopic structure of this mysterious phase has been debated for a long time.

In fact, at least two different rippled states have been reported, which often coexist [10]. Electron density maps (EDMs) have recently been derived for both of them from x-ray scattering data [11,12]. One of the structures is asymmetric and has a sawtooth profile with alternating thin and thick arms and a periodicity of 13–15 nms, which corresponds to roughly 20 lipid diameters. The other one is symmetric and has a wavy sinusoidal structure with twice the period of the asymmetric structure [13]. The formation of the ripples depends strongly on the thermal history [10,13,14]. If the membrane is heated up from the gel state, asymmetric ripples are obtained. If one cools down from the fluid state, both types of ripples are formed—predominantly asymmetric ones if the cooling was fast, and predominantly symmetric ones if the cooling was slow and if a long time was spent at the transition temperature. Dynamical x-ray [13] and atomic force microscope [15] studies suggest that the symmetric ripple state is metastable and very slowly transforms into the asymmetric ripple state; however, this does not yet seem to be fully settled. The degree of ordering in the ripple states largely resembles that in the gel state, except for a certain amount of disorder in the structure: calorimetric studies suggest that approximately 10% of all chains are melted. Most strikingly, the self-diffusion of lipids in the ripple states is a few orders of magnitude higher than that in the gel state, and highly anisotropic [16]. This has lead to the assumption that the ripple states might contain "coexisting" gel-state and fluid-state lipids.

Numerous theoretical models for the ripple phase have been proposed, which explain the ripple formation by different mechanisms: Chain packing effects [17,18], dipolar interactions [19], a coupling of monolayer curvature with local chain melting [20–22] or with tilt [17,23,24] in combination with chirality [24]. This list is far from complete. In contrast, molecular simulations of rippled membrane states are still scarce. Kranenburg *et al.* [25] were the first to reproduce a periodically modulated membrane state in a dissipative-particle dynamics simulation of a coarse-grained lipid model. They observe a periodic sequence of stripes with alternating gel and liquid order, similar to a

structure proposed theoretically by Falkovitz *et al.* [20]. Unfortunately, the distribution of head groups in that structure is not consistent with the experimental EDMs: the structure is neither asymmetric, nor does it feature the waviness which characterizes the symmetric ripple. Moreover, the relative fraction of molten molecules, 50%, seems too high compared with experiments. A second, very interesting simulation has recently been carried out by de Vries *et al.* [26]. In an atomistic model of a lecithin bilayer, these authors found a structure containing a stretch of interdigitated membrane and a stretch of gel membrane. The interdigitated patch connects the neighboring gel membrane such that the upper leaflet of the bilayer on one side crosses over into the lower leaflet on the other side. The authors assume that this structure will repeat itself periodically in larger systems and identify it with an asymmetric ripple. It is worth noting that the lipids are not arranged in a continuous bilayer, as had been assumed in all previous models for the ripple state.

In this Letter, we present Monte Carlo simulations of a simplified coarse-grained lipid model, which reproduce asymmetric and symmetric ripple states with properties that compare very favorably to experiments. The structure of the asymmetric ripple is similar to that proposed by de Vries *et al.* [26]. Our simulations show that it is indeed a periodic structure, and that it is generic; i.e., it does not depend on molecular details of the lipids. Moreover, they enable us to propose a structural model for the symmetric ripple as well, and to identify the mechanisms that stabilize the rippled structures.

We employ a lipid model which we have used earlier to investigate phase transitions in Langmuir monolayers [27,28]: Lipid molecules are represented by chains made of one head bead and six tail beads [Fig. 1(b)], which are connected by anharmonic springs and subject to an intramolecular bending potential. The tail beads attract one another with a truncated and shifted Lennard-Jones potential (diameter σ, well depth $\sim\epsilon$). The head beads are larger than the tail beads (1.1σ) and purely repulsive. The other parameters and the exact form of the potentials can be found in Ref. [28] (the model corresponding to Fig. 7). Self-assembly of the ''lipids'' is enforced with a recently proposed ''phantom solvent'' environment [29]: We add ''solvent'' particles which interact only with lipid beads (repulsively), and not with one another. Two examples of self-assembled membranes in the L_α and the $L_{\beta'}$ state are shown in Figs. 1(c) and 1(d). The phantom solvent has the simple physical interpretation that it probes the accessible free volume for solvent particles in the presence of lipids. It entropically penalizes lipid-solvent interfaces, and thus effectively creates an attractive ''depletion'' interaction between the lipid beads next to such an interface, i.e., the head beads [30]. The strength of this interaction is directly proportional to the phantom solvent density, ρ_s. Compared with other explicit solvent environments, the phantom solvent has the advantage that it does not introduce an artificial solvent structure and artificial solvent-mediated interactions between periodic images of bilayers. Moreover, it is computationally cheap: in Monte Carlo simulations, less than 10% of the total computer time is typically spent on the uninteresting solvent region.

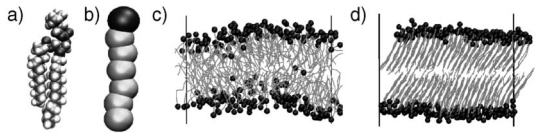

FIG. 1. Illustration of our lipid model and snapshots (side view) of two lipid states (at $\rho_s k_B T = 2\epsilon/\sigma^3$). (a) All-atom model of dipalmitoyl phosphatidylcholine (DPPC); (b) coarse-grained bead-spring model used in this Letter; (c) the fluid phase L_α at $k_B T = 1.3\epsilon$; (d) the tilted gel phase $L_{\beta'}$ at $k_B T = 1.1\epsilon$. Only heads (reduced size) and tail bonds are shown.

We have carried out Monte Carlo simulation at constant pressure with periodic boundaries in a simulation box of fluctuating size and shape. This ensured that the membranes had vanishing surface tension. The system sizes ranged from 288 to 1800 lipids, typical run lengths were $1–10 \times 10^6$ Monte Carlo sweeps. The resulting phase diagram is shown in Fig. 2. The model reproduces the experimentally observed gel and fluid phases for lipids with large heads: the fluid phase (L_α), the interdigitated gel (L_β^{int}) for low ρ_s, i.e., weak head attraction, and the tilted gel ($L_{\beta'}$) for higher ρ_s, i.e., strong head attraction. The structures of these phases and the phase transitions shall be discussed in detail elsewhere [31].

Here, we fix the solvent density at $\rho_s k_B T = 2\epsilon/\sigma^3$, where the gel phase has the tilted $L_{\beta'}$ structure. In the

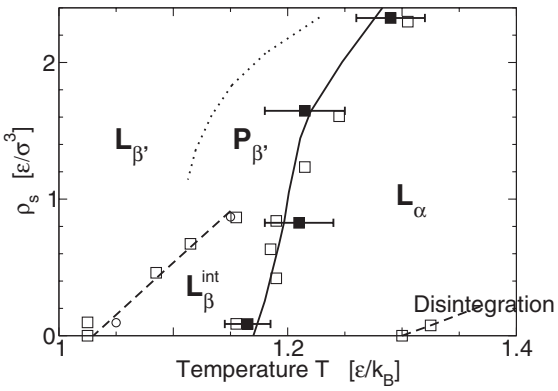

FIG. 2. Phase diagram of the lipid model as a function of temperature T and phantom solvent density, i.e., effective head interaction ρ_s. The phases are as follows: L_α (fluid), $L_{\beta'}$ (tilted gel), L_β^{int} (interdigitated gel), P'_β (ripple). At high temperatures, the bilayer disintegrates. Open squares indicate transition points from simulation runs of small systems initially set up as fully ordered, untilted bilayers. No ripples were observed in that case. Solid squares show transition points determined by heating up and cooling down the system (different system sizes), with the error bars corresponding to the width of the hysteresis. Open circles denote points where the membrane undergoes a transition from $L_{\beta'}$ to L_β^{int} upon heating.

transition region between $L_{\beta'}$ and L_α, we observe modulated configurations which we identify with rippled states. They develop spontaneously and reproducibly when cooling a fluid membrane or heating a tilted gel membrane in a temperature range close to the transition temperature. As in the experiments, their exact structure depends on the thermal history. Figure 3 (left) shows three examples.

The structure in Fig. 3(a) emerged after cooling the system rapidly from the fluid phase down to $k_BT = 1.1\epsilon$. It exhibits two ripples of width $\sim 15\sigma$ with a structure very similar to that found by de Vries *et al.* [26] in their atomistic simulations: At each ripple, a thin interdigitated line defect connects a lower with an upper monolayer. The second monolayer ends at that line with an edge of disordered, melted chains. The period, $\sim 15\sigma$, corresponds to the "natural" period of asymmetric ripples in our model. This was deduced by comparing simulations of systems with different sizes. The quality of the ripple formation depends on the initial box dimensions (before cooling). In systems of half the size, only one ripple formed. If one box dimension was close to a multiple of 15σ, the box shape readjusted to accommodate the optimal ripple width. If the initial box dimensions were very unfavorable (20 or 24σ), no clean ripples formed; instead, the ripples bulged and developed interconnected structures.

The second structure, shown in Fig. 3(b), resulted from heating up a bilayer in the tilted gel state up to a temperature close to the main transition, $k_BT = 1.21\epsilon$. During the simulation, the bilayer first fluctuated very strongly. After $\sim 6 \times 10^6$ Monte Carlo sweeps, the tilt was so strong that the lipids in both monolayers slid along each other and connected with the other monolayer. The final structure exhibited one asymmetric ripple and fluctuated much less. This structure remained stable for another 6×10^6 sweeps. Apparently, the formation of the second ripple is prevented kinetically.

The third structure, Fig. 3(c), shows a membrane which has been cooled down from the fluid state to a temperature close to the main transition $k_BT = 1.18\epsilon$. In this case, a new type of structure emerged: The membrane maintains its bilayer structure, but the monolayers contain curved, ordered stripes with a width of roughly 25σ. These gel stripes on the upper and lower monolayers are interlocked, such that the membrane assumes an overall sinusoidal shape. Each stripe ends on both sides with conical regions of disordered chains, which are very similar to the monolayer caps in the asymmetric ripple state. The total width of a ripple is $\sim 30\sigma$, which is twice as much as the width of an asymmetric ripple. We identify this structure with the symmetric ripple state.

To support this hypothesis, we superimpose the proposed structures for the asymmetric and the symmetric ripple with the EDMs of Sengupta *et al.* [12] in Fig. 4. They can be inserted very nicely. In the asymmetric case, they explain the sawtooth shape with the thin and thick arm (assuming that the interdigitated region is indeed small). In the symmetric case, they reproduce the sinusoidal shape.

The simulations can be used to characterize the ripple states in more detail. We just summarize some of the results here, the data will be presented and discussed elsewhere [31]. The structure of the ripple states is in many

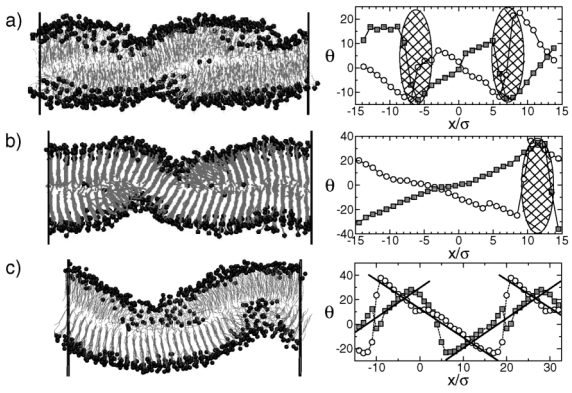

FIG. 3. Three examples of ripple configurations in a model bilayer of 720 molecules (left) with corresponding tilt profiles $\theta(x)$ (right). (a) Two asymmetric ripples, formed after rapidly cooling down to the temperature $k_BT = 1.1\epsilon$ from the L_α phase; (b) one asymmetric ripple, formed after heating up to $k_BT = 1.21\epsilon$ from the $L_{\beta'}$ phase; (c) symmetric ripple, formed after slowly cooling down to the temperature $k_BT = 1.18\epsilon$ from the L_α phase. Note that the snapshots (left) show side views of whole fluctuating configurations; therefore, a large number of heads seem to be buried inside the layer, even though they are at the surface. The curves in the graphs (right) are shifted in the x direction and replicated periodically. Open circles correspond to the lower monolayer, solid squares to the upper monolayer. The hatched ellipses indicate the regions with the interdigitated line defect, and the thick solid lines in (c) the slopes of θ on the ordered monolayer regions.

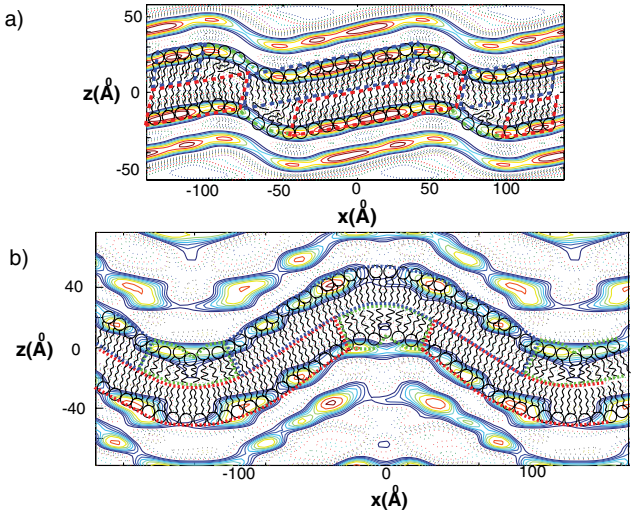

FIG. 4 (color online). Sketch of the proposed microscopic structures for the ripple states layers superimposed onto EDMs from Ref. [12]. (a) Asymmetric ripple (on an EDM for dimyristoyl phosphatidylcholine at 18.2 °C); (b) symmetric ripple (on an EDM for DPPC at 39.2 °C).

respect similar to that of a gel: Roughly ~85% of the chains have chain lengths distributed as in the gel, only 15% have a reduced length. This is in rough agreement with the experimental findings on the amount of chain disorder in the ripple state. The head layer in the ordered parts of the ripple state has the same thickness than in the gel state. The structure factor of the ripple state indicates a large amount of positional order, and resembles that of an untilted gel. The most revealing structural feature is the average tilt of the molecules. It points perpendicular to the ripple and is modulated. Figure 3 (right) shows profiles of the average tilt angle θ for the three ripples discussed above. The slope $\theta'(x)$ turns out to be almost constant throughout the whole ordered part of the monolayer. Moreover, the numerical values are comparable: $\theta' \sim 2.6/\sigma$ on average for the two asymmetric ripples, and $\theta' \sim 2.5/\sigma$ for the symmetric ripple. Even the single asymmetric ripple of Fig. 3(b), which has an unfavorable period, still features a constant slope of $\theta' \sim 2.3/\sigma$. This suggests strongly that the ripple formation is primarily driven by the propensity of lipids with large head groups to exhibit splay. The driving force of the local curvature, i.e., head packing, is much weaker. It does, however, play a role in determining the periodicity of the ripple. Our cooling simulations clearly indicate that the system favors a certain ripple width, for which both splay and curvature are optimized.

In sum, we have reproduced symmetric and asymmetric rippled states with a generic model for lipid membranes. The comparison with experiments is favorable: The structure is consistent with the available EDMs, the period length is of the same order as the experimental period length (~15 lipid diameters), the amount of chain disorder is comparable, and we observe the same dependence on thermal history. Therefore, we believe we have strong evidence that our structures correspond to the real ripple states observed in experiments. Factors that are important for the formation of these states are the following: (i) the vicinity to the L_α phase, such that a small number of chains can melt; (ii) a strong tendency of monolayers to splay inwards, caused by a mismatch between head group and tail size; and (iii) the possibility to interdigitate. Chirality is not necessary, in agreement with experiments [13]; the lipids do not even have to be asymmetric.

In fact, the factor (iii) is needed only to stabilize the asymmetric ripple state. If it is absent, the system can still form a symmetric ripple state. We note that the symmetric and the asymmetric ripples are structurally quite similar. Both contain about the same amount of molten chains, both have large ordered monolayer regions with comparable splay. This explains why the two types of ripples coexist, and why it seems so hard to determine which one is stable. Our results suggest that the answer to that question may depend on the type of lipid, e.g., on the head interactions and other factors that promote or prevent interdigitation. Coarse-grained lipid models may help to study this systematically. Unfortunately, we have not yet been able to develop an efficient strategy to determine the free energy difference between the two states. This will be subject of future work.

We thank V. A. Raghunathan for providing us with the EDMs, and the NIC computer center Jülich for computer time. This work has been funded by the Deutsche Forschungsgemeinschaft within the SFB 613.

[1] R. B. Gennis, *Biomembranes* (Springer-Verlag, Berlin, 1989).
[2] J. F. Nagle, Annu. Rev. Phys. Chem. **31**, 157 (1980).
[3] J. F. Nagle and S. Tristram-Nagle, Biochim. Biophys. Acta **1469**, 159 (2000).
[4] R. Koynova and M. Caffrey, Chem. Phys. Lipids **69**, 1 (1994).
[5] R. Koynova and M. Caffrey, Biochim. Biophys. Acta **1376**, 91 (1998).
[6] In general, lipids are ester linked. By changing the chain linkage type from ester to ether, one removes a strong hydrogen bond acceptor, which reduces the tendency of head groups to form hydrogen bonds with one another.
[7] F. Schmid and M. Schick, J. Chem. Phys. **102**, 2080 (1995).
[8] M. D. Whitmore, J. P. Whitehead, and A. Roberge, Can. J. Phys. **76**, 831 (1998).
[9] A. Tardieu, V. Luzzati, and F. C. Reman, J. Mol. Biol. **75**, 711 (1973).
[10] B. G. Tenchov, H. Yao, and I. Hatta, Biophys. J. **56**, 757 (1989).
[11] W. J. Sun *et al.*, Proc. Natl. Acad. Sci. U.S.A. **93**, 7008 (1996).
[12] K. Sengupta, V. A. Raghunathan, and J. Katsaras, Phys. Rev. E **68**, 031710 (2003).
[13] J. Katsaras *et al.*, Phys. Rev. E **61**, 5668 (2000).
[14] S. Matuoka *et al.*, Biophys. J. **64**, 1456 (1993).
[15] T. Kaasgaard *et al.*, Biophys. J. **85**, 350 (2003).
[16] M. B. Schneider, W. K. Chan, W. W. Webb, Biophys. J. **43**, 157 (1983).
[17] K. Larsson, Chem. Phys. Lipids **20**, 225 (1977).
[18] P. A. Pearce and H. L. Scott, J. Chem. Phys. **77**, 951 (1982).
[19] S. Doniach, J. Chem. Phys. **70**, 4587 (1979).
[20] M. S. Falkovitz *et al.*, Proc. Natl. Acad. Sci. U.S.A. **79**, 3918 (1982).
[21] M. Marder *et al.*, Proc. Natl. Acad. Sci. U.S.A. **81**, 6559 (1984).
[22] T. Heimburg, Biophys. J. **78**, 1154 (2000).
[23] J. M. Carlson and J. P. Sethna, Phys. Rev. A **36**, 3359 (1987).
[24] T. C. Lubensky and F. C. MacKintosh, Phys. Rev. Lett. **71**, 1565 (1993).
[25] M. Kranenburg, C. Laforge, and B. Smit, Phys. Chem. Chem. Phys. **6**, 4531 (2004).
[26] A. H. de Vries *et al.*, Proc. Natl. Acad. Sci. U.S.A. **102**, 5392 (2005).
[27] C. Stadler, H. Lange, and F. Schmid, Phys. Rev. E **59**, 4248 (1999).
[28] D. Düchs and F. Schmid, J. Phys. Condens. Matter **13**, 4853 (2001).
[29] O. Lenz and F. Schmid, J. Mol. Liq. **117**, 147 (2005).
[30] Free head beads and solvent demix at $\rho_s \sim 2.6/\sigma^3$.
[31] O. Lenz and F. Schmid (to be published).